Experimental Investigation and Numerical Simulation of the Heating/Cooling Process in Rotational Molding Enhanced with Fins

Shih-Jung Liu, Kwang-Hwa Fu

Polymer Rheology and Processing Lab, Department of Mechanical Engineering, Chang Gung University, Tao-Yuan 333, Taiwan

Received 12 October 2006; accepted 23 July 2007
DOI 10.1002/app.27294
Published online 29 January 2008 in Wiley InterScience (www.interscience.wiley.com).

ABSTRACT: Rotational molding has become one of the most important polymer processing methods for producing hollow plastic articles. However, the long-cycle time required by the rotational molding process has confounded the overall success of this technology. Molds with extended surfaces (fins) have the potential to enhance heat transfer by increasing surface area. This report aims to investigate, both experimentally and numerically, the heating/cooling process of rotational molds enhanced with fins. Rotational molding experiments were carried out in a laboratory scale uniaxial machine, which is capable of measuring internal air temperature in the cycle. Molds enhanced with three types of fins, including pin, rectangular, and triangular fins, were used to manufacture the parts. It was found that the mold surface enhanced with pins exhibited the highest heating and cooling rate. Nevertheless, from a design perspective, ease of manufacturing needs to be taken into account which could make triangular fin geometry a better choice to enhanced heat transfer. In addition, an unsteady-state, nonlinear heat transfer model of rotational molding has been proposed to numerically simulate the internal air temperature profiles. It is shown that the numerical predictions are in good agreement with experimental data. This model enables prediction of the heating and cooling time of rotational molding enhanced with fins, and hence the overall cycle time for the process. © 2008 Wiley Periodicals, Inc. J Appl Polym Sci 108: 1696–1705, 2008

Key words: rotational molding; fins; heating/cooling process; experiments; numerical simulation

INTRODUCTION

Rotational molding has been one of the most important polymer processing methods for producing hollow plastic articles.[1] The plastic powder is placed in one half of a mold. The mold is then closed and subjected to biaxial rotation in an oven with a heating temperature of 200–400°C. The plastic powder inside the mold is melted by heat transferred through the mold wall. When all the powder has melted, the mold is moved out of the oven while maintaining the biaxial rotation. Still air, a blowing fan, or water shower is usually used to cool the mold. Once the product inside the mold is cooled to a state of sufficient rigidity, which in most cases occurs when all regions of the part have cooled to below the melting temperatures of the polymers, the mold opens and the product is removed.

Rotational molding offers design advantages over other molding processes. With proper design, parts that are assembled from several pieces can be molded as one part, eliminating expensive fabrication costs. The process also has a number of inherent design strengths such as a consistent wall thickness and strong outside corners that are virtually stress-free. If additional strength is required, reinforcing ribs can be designed into the part. Inserts, threads, handles, minor undercuts, and flat surfaces that eliminate draft angles or fine surface detail can all be part of the design. Designers also have the option of multiwall molding that can be either hollow or foam filled. When cost is a factor, rotational molding has an advantage over other types of processes as well. In comparison to injection and blow molding, rotational molding can easily produce large and small parts in a cost effective manner. Tooling is less expensive because there is no internal core to manufacture. Since there is no internal core, minor changes can be easily made to an existing mold. Furthermore, because parts are formed with heat and rotation, rather than pressure, molds do not need to be engineered to withstand the high pressure of injection molding. Production costs for product conversions are reduced because lightweight plastics replace heavier, often more costly materials. This makes rotational molding as cost effective for one-of-a-kind prototypes as it is for large production runs.[2–6]

Correspondence to: S.-J. Liu (shihjung@mail.cgu.edu.tw).
Contract grant sponsor: National Science Council of Taiwan, R.O.C; contract grant number: NSC95-2221-E-182-032-MY3.

Despite the advantages associated with the rotational molding process, there are still some unsolved problems that limit the applications of this technology. The long-cycle time caused by the low heating/cooling efficiencies of the molding process is one of them. Molds enhanced externally by fins have the potential to facilitate the heat transfer and reduce the cycle time by increasing the surface areas. Despite the fact that this rotational molding technique has been developed for over three decades, research efforts on rotational molds with extended surfaces[7] have been limited. In addition, although various models have been proposed[8–10] to simulate the rotational molding process, no paper has addressed the simulation of rotational molds enhanced with fins.

This report, following up the work done by Bickerton's group[7] on molds with extended surfaces, aims to investigate both experimentally and numerically, the heating/cooling process of rotational molds enhanced with fins. Rotational molding experiments were carried out in a laboratory scale uniaxial machine, which is capable of measuring internal air temperature in the cycle. Three types of fin-enhanced molds, including pin, rectangular, and triangular fins, were used to manufacture the parts. In addition, an unsteady-state, nonlinear heat transfer model of the rotational molding has been proposed to numerically simulate the internal air temperature profiles. The model parameters are determined from differential scanning calorimetry measurements. The results of this study will enable prediction of the heating and cooling time of rotational molding enhanced with fins, and hence the overall cycle time for the process. This model would provide significant advantages in terms of reduced cycle time and improved product quality.

EXPERIMENTAL

Materials

The resin used in this study was linear low-density polyethylene (LLDPE). The melt flow index of the polymer was measured at 5.0. The measurement was conducted on a Kayness melt flow indexer, according to ASTM D1238 standard. The resin was available in spherical particles with a diameter around 3 mm, and was ground into powder by a local grinding agent.

Rotational molding setup

One laboratory-scale uniaxially rotating machine was designed and built in our laboratory. It consisted of a mold rotating arm and an electrically heated oven with a circulation fan (Fig. 1). A $100 \times 100 \times 165$ mm^3 box mold made of a 7-mm thick sheet of aluminum was used for the molding tests. Four base plates with a thickness of 5mm enhanced with three types of fins—pin, rectangular, and triangular fins (Fig. 2) were mechanically attached to the surface of the box mold (Fig. 1) to form the fin enhanced molds. The volume and surface areas of the initial mold, excluding the two sides of the mold along the rotating axis which are heat insulated, are 429,660 and 66,000 mm^2, respectively. All three types of fins have comparable volumes but different surface areas (Table I). The percentage increase in volume and surface of the mold with addition of fins is also listed in Table I. The oven temperatures ranged between 250 and 500 °C. Preweighed powder quantities were placed inside the mold. The mold rotation speed was set and the mold was then moved into the oven.

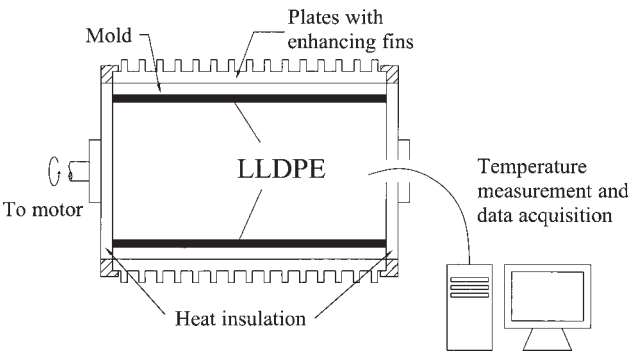

Figure 1 Schematically, the rotational molding setup, the mold, the thermocouple, and the data acquisition.

In-mold air temperature measurement

During the molding process, the internal mold (air) temperature was recorded by a 1.6-mm sheath diameter grounded thermocouple through the venting (Fig. 1). The thermocouple was connected to a personal computer through an RS-232 interface. The temperature profiles were recorded by LabVIEW (National Instrument, USA) data acquisition software.

DSC measurement

The melting and crystallization of the polymeric materials were studied by differential scanning calorimeter (DuPont model TA 2000). The measurement of enthalpy was carried out at a heating and a cooling rate of 10°C/min.

NUMERICAL SIMULATION OF HEAT TRANSFER

Transient heat transfer model

An unsteady state, nonlinear heat transfer model is proposed in this study to predict the temperature of the in-mold air during the whole rotational molding

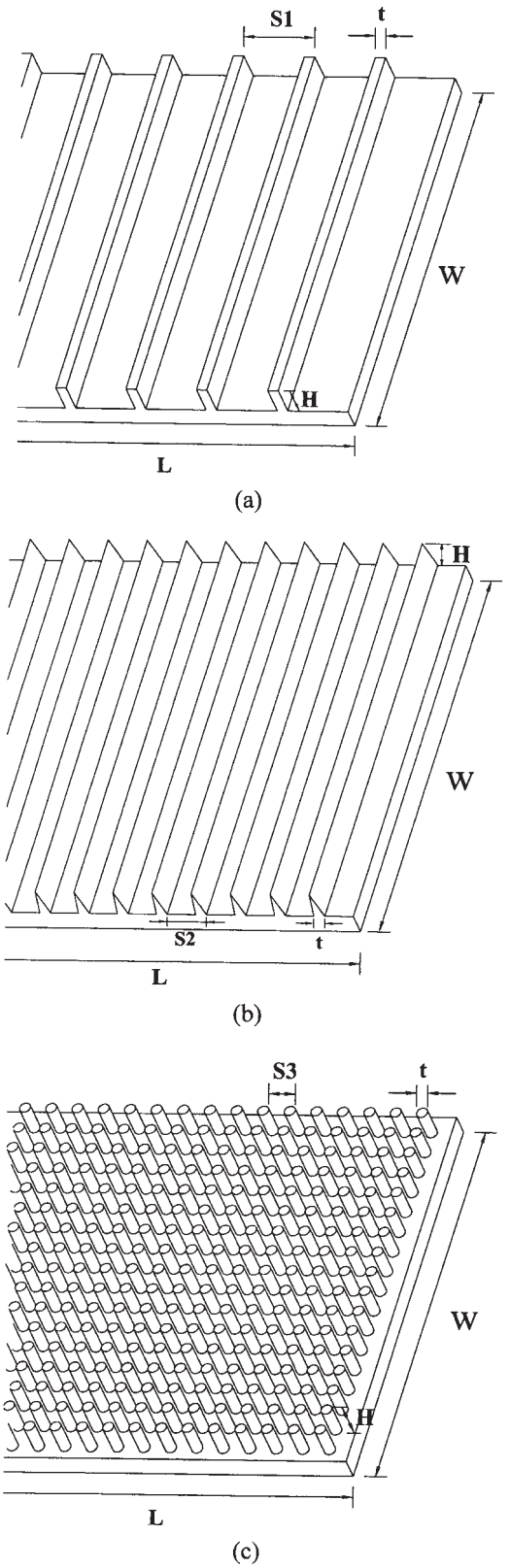

Figure 2 Various fins (a) rectangular fin, (b) triangular fin, and (c) pin fin used to enhance the rotational molds (thickness of the base plates is 5 mm, $t = 2.47$ mm, $H = 7$ mm, S1 = 16.75 mm,W = 93mm, S2 = 8.8 mm, L = 165 mm, and S3 = 6 mm).

TABLE I
The Volumes and Surface Areas of Various Fins

Fin type	Rectangular fin	Triangular fin	Pin fin
Total surface area (mm^2)	112,872	140,044	159,858
Percentage increase in surface area (%)	71	112.2	142.2
Total volume (mm^3)	797,493	800,044	801,661
Increase in total volume (%)	85.6	86.2	86.6

[a] Materials used to make the mold are aluminum alloy with a density of 2790 kg/m^3.
[b] The surface area and the volume of the initial mold are 66,000 and 429,660 mm^3, respectively.

process. For simplicity reasons, the modeling of the rotational molding for parts of any geometry is divided into three distinct stages, as shown schematically in Figure 3. Stage 1 represents the so-called induction (heating of powder) and polymer sintering (melting and sintering). The mold is heated while rotating. The available plastic powder is deposited throughout the mold and is assumed to be stagnant. Stage 1 is defined as lasting until the inside wall temperature of the mold reaches the melting temperature of the plastic. The modeling of the heating condition in this stage can be as described in Figure 4(a). Stage 2 represents the so-called fusion of the material (heating of polymer melt and bubble dissolution). In this stage there is essentially no plastic migration due to the high viscosity of the molten plastic. The heat transfer in this stage can be modeled as shown in Figure 4(b). Stage 2 ends when the in-mold temperature reaches the expected peak temperature. Stage 3 includes the cooling of the melt, melt solidification, and cooling of the polymer solid. The modeling of the heat transfer process is as shown in Figure 4(c).

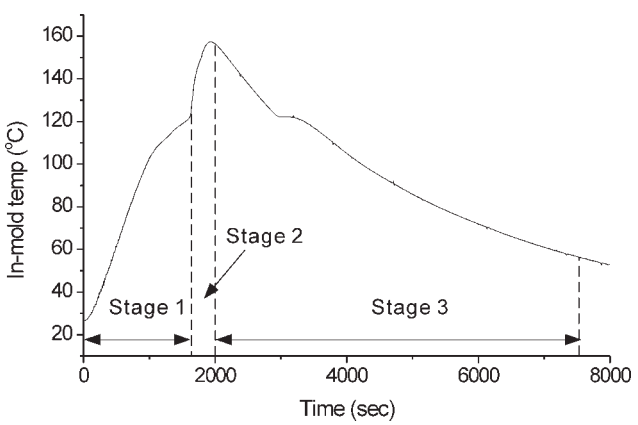

Figure 3 Schematically, a typical internal air temperature profile of the rotational molding process and its modeling by three different stages.

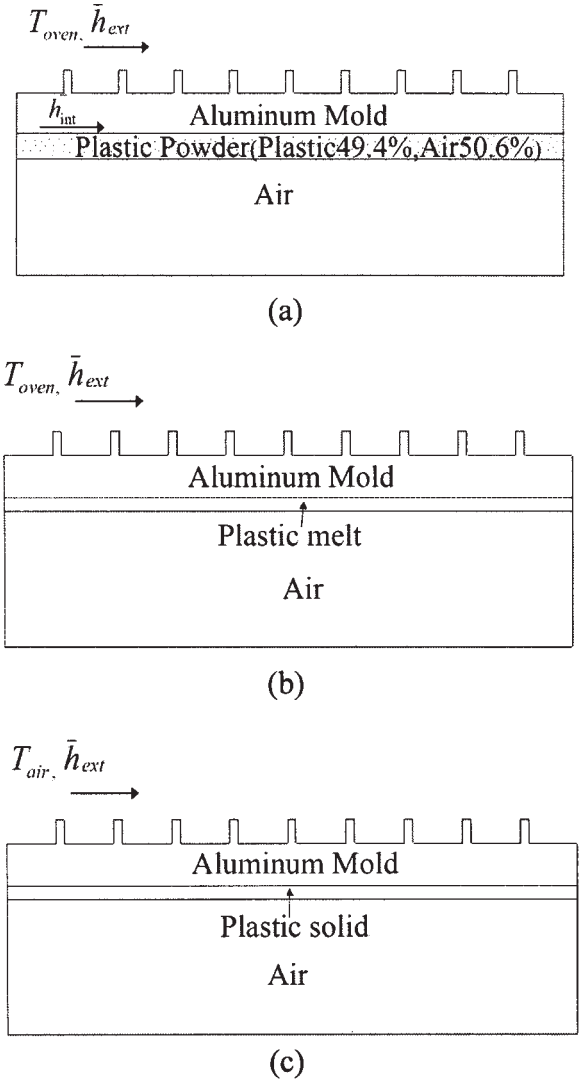

Figure 4 Schematically, the modeling of the heating and cooling of the rotational molding process (from a to c for Stages 1 to 3, respectively).

The heat transfer analysis[11] begins from the energy balance of the system, i.e.,

$$\rho C_p \frac{dT}{dt} = k\nabla^2 T + Q \tag{1}$$

where ρ is the density, C_p is the heat capacity, k is the thermal conductivity of the materials, and Q is the volumetric heat source. After derivation of the formulations by using the weight residual methods,[12,13] the following expression ready for numerical simulation can be obtained,

$$[\mathrm{C}]\{\dot{\mathrm{T}}\} + [\mathrm{K}]\{\mathrm{T}\} = \{\mathrm{F}_v\} + \{\mathrm{F}_s\} \tag{2}$$

with

$$[\mathrm{K}] = \int_\Omega [\mathrm{B}]^T k[\mathrm{B}]dV \tag{3}$$

$$[\mathrm{C}] = \int_\Omega [\mathrm{N}]^T \rho C_p[\mathrm{N}]dV \tag{4}$$

$$\{\mathrm{F}_v\} = \int_\Omega [\mathrm{N}]Q dV \tag{5}$$

$$\{\mathrm{F}_s\} = \int_\Omega [\mathrm{N}]^T q dV \tag{6}$$

where [N] is the shape function (interpolation function) matrix and [B] is the shape function derivative matrix. The shape function is a matrix that describes how the temperature at one specific position is interpolated from nodal temperatures over the elements. The shape functions[12] for the 2D isoparametric elements are,

$$\begin{aligned} N_1 &= \frac{1}{4}(1-\xi)(1-\eta) \\ N_2 &= \frac{1}{4}(1+\xi)(1-\eta) \\ N_3 &= \frac{1}{4}(1+\xi)(1+\eta) \\ N_4 &= \frac{1}{4}(1-\xi)(1+\eta) \end{aligned} \tag{7}$$

Details on the derivation of the shape function [N] for various elements can be found in the reference.[12] By introducing the finite difference discretization into eq. (2),

$$\{\mathrm{T}\} = \Theta\{\mathrm{T}\}^{t+\Delta t} + (1-\Theta)\{\mathrm{T}\}^t \tag{8}$$

we can get the following equations for iteration,

$$\begin{aligned} ([\mathrm{C}] + \Theta\Delta t[\mathrm{K}])\{\mathrm{T}\}^{t+\Delta t} = ([\mathrm{C}] - (1-\Theta)\Delta t[\mathrm{K}])\{\mathrm{T}\}^t \\ + (\{\mathrm{F}_v^*\} + \{\mathrm{F}_s^*\})\Delta t \end{aligned} \tag{9}$$

with

$$\{\mathrm{F}_v^*\} = \Theta\{\mathrm{F}_v\}^{t+\Delta t} + (1-\Theta)\{\mathrm{F}_v\}^t \tag{10}$$

$$\{\mathrm{F}_s^*\} = \Theta\{\mathrm{F}_s\}^{t+\Delta t} + (1-\Theta)\{\mathrm{F}_s\}^t \tag{11}$$

With the initial temperatures given and the boundary conditions assigned, the numerical iteration provides the air temperature distribution inside the mold at different elapsed times.

Boundary and initial conditions

Before numerical calculation of the problem, the different boundary conditions (BC) at the interface of regions characterized by different material properties

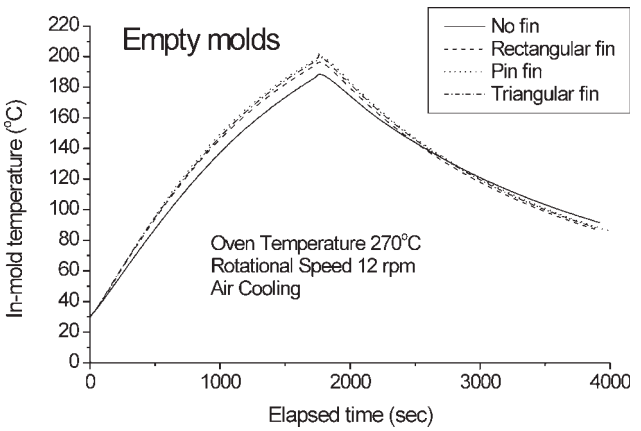

Figure 5 In-mold air temperatures carried out on empty molds with various fins.

need to be assigned. The BC at the external mold surface, in contact with the heating gases into the oven, has been assumed to be governed by convection:

$$q_{\text{ext}} = \bar{h}_{\text{ext}}(T_{\text{mold}} - T_{\text{oven}}) \tag{12}$$

To estimate $\bar{h}_{\text{ext}}$, a few test trials were completed on the empty mold of various fins. Figure 7 shows the measured in-mold air temperature profiles. The heat transfer model was used to simulate the in-mold air temperatures of the empty mold experiments in Figure 5 for various fins. The heat convection coefficients $\bar{h}_{\text{ext}}$ thus obtained are listed in Table II. The results in Table II suggest that the heat convection coefficients of the finned molds are smaller than that of the initial (nonfinned) mold. This might be due to the fact that the total thickness of the finned molds (12 mm) used in this study is thicker than that of the initial mold (7 mm). Internally, before the complete melting of the polymer powder, the flow of solid polymer particles in the mold is neglected, following the assumption made by other researchers[8–10] when modeling this process and which has led to predictions that match well experimental results. Furthermore, the heat transfer from the mold to the powder is assumed to be governed by heat convection:

$$q_{\text{int}} = \bar{h}_{\text{int}}(T_{\text{mold}} - T_{\text{powder}}) \tag{13}$$

It has been reported by Olson et al.[10] that the simulation results were relatively insensitive to $\bar{h}_{\text{int}}$. Therefore, the value of $\bar{h}_{\text{int}} = 2\ \text{W/m}^2\ ^\circ\text{C}$ was chosen[10] for all molds with various fins in the analysis.

After the complete melting of the polymeric powders, the BC at the internal mold surface has been assumed to be controlled by conduction. It is assumed that for most of the process, the polymer in contact with mold forms a film at the mold surface. In these conditions, the very high melt viscosity in practice prevents any relative motion of the material on the mold wall, thus avoiding convective heat transfer. The heat transfer from the mold to the polymer melt film (or solid layer during the cooling process) to the internal air is assumed to be governed by heat conduction.

For the remainder of the simulations, we simply varied the geometry of the fins and included the plastic materials. Other parameters were held constant. Finally, the initial temperatures of mold, polymer, and air in Eq. 2 are assumed to be at a room temperature of 25°C.

Parameter determination

The proposed heat transfer model given in eq (2) requires the use of proper equations to model the phase transitions of a rotational molding grade LLDPE. To determine the heat source term in eq (2), the melting and crystallization of LLDPE were studied through differential scanning calorimetry (DSC). Figure 6(a) shows the DSC curve of the melting process. For the material properties in Stage 1, the density ρ, heat capacity C, and thermal conductivity k of the polymer powder can be determined by the following equations:[8,9]

$$\rho = \rho_{\text{polymer}} \cdot \text{vp} + \rho_{\text{air}} \cdot (1 - \text{vp}) \tag{14}$$

$$C = C_{\text{polymer}} \cdot \text{vp} + C_{\text{air}} \cdot (1 - \text{vp}) \tag{15}$$

$$k = k_{\text{polymer}} \cdot \text{vp} + k_{\text{air}} \cdot (1 - \text{vp}) \tag{16}$$

where vp is the volume percentage of the polymer inside the powder and is determined to be 49.4% by using the apparent density measurement method in ASTM D1895-69. Furthermore, the enthalpy H of the polymer powder during the melting process can be calculated based on the following equations:

$$C^* = C + L_f/\Delta T \tag{17}$$

$$H = \rho^* C^* \Delta T \tag{18}$$

and the result is shown in Figure 6(b) and Table III. On the other hand, despite there may be some air

TABLE II
The External Heat Convective Coefficient Used for Various Fins

Fin type	$\bar{h}_{\text{ext}}$ (W/m^2 °C) for heating	$\bar{h}_{\text{ext}}$ (W/m^2 °C) for cooling
No fin	19	13.6
Rectangular	12	9.6
Pin	8	6
Triangular	9.5	7.8

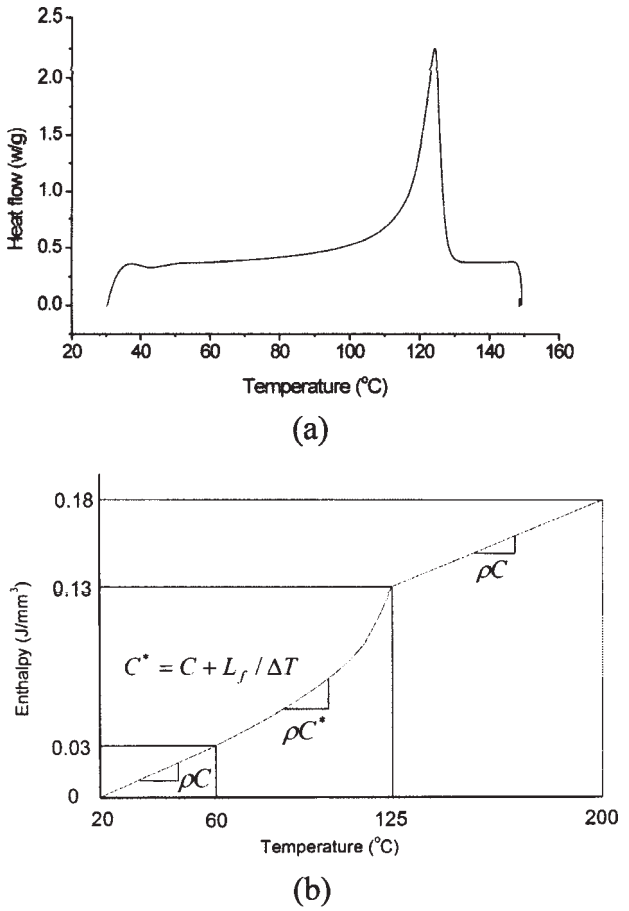

Figure 6 (a) DSC curve of the polymeric materials during melting, and (b) enthalpy of the materials at various temperatures.

trapped in the polymer layer (either dissolved or in the form of bubbles), its effect on the heat transfer is limited and thus neglected. The enthalpy of the cooling crystallization in Stage 3 is directly obtained from the DSC curves in Figure 7 and the result in listed in Table IV.

TABLE III
Enthalpy of the Polymeric Materials During the Melting Process

Temperature range (°C)	Heat of fusion (J/kg)	$L_f/\Delta T$ (J/kg °C)
60–65	1400	280
65–70	1500	300
70–75	1700	340
75–80	2400	480
80–85	2740	548
85–90	3250	650
90–95	3910	782
95–100	5120	1024
100–105	6720	1344
105–110	9130	1826
110–115	13,880	2776
115–120	26,700	5340
120–125	29,650	5930

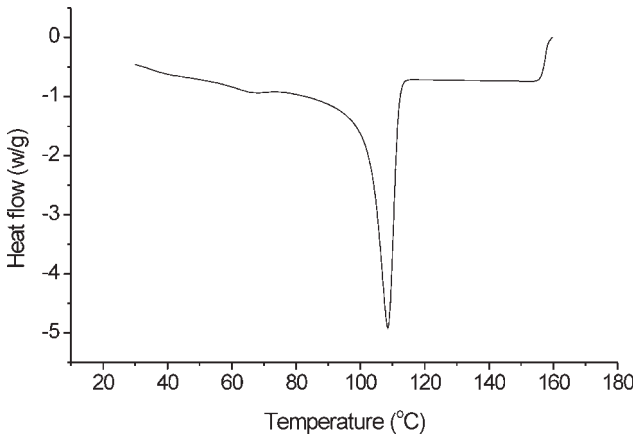

Figure 7 DSC curve of the polymeric curve during cooling.

Finite element calculation

A box mold with various fin geometries on its surface was examined and modeled. The transient heat transfer analysis of the rotational molding process was completed by employing a commercially available program ANSYS 5.3 (Swanson, New Jersey, USA). A 2D model was used to simulate the mold geometry with rectangular and triangular fins, while a 3D model was used for the mold with pin fins. The thermophysical properties[11] used for aluminum, polyethylene, and air were listed in Tables V and VI, respectively. Linear interpolations were used to predict the properties between various temperatures. With an initial melt temperature given; the transient heat transfer analysis was carried out to obtain the in-mold air temperature distributions at different times.

RESULTS AND DISCUSSION

Internal air temperature profiles and fin selection

The internal mold temperature profiles were recorded during the heating and cooling cycle, by

TABLE IV
Enthalpy of the Polymeric Materials During the Crystallization Process

Temperature (°C)	Heat capacity (J/kg °C)
30	1285.71
50	2300
90	3284.41
95.3	3787.01
99.4	4792.2
102.05	5766.23
103.8	6740
108.6	14902.6
113.63	2300
150	2300

TABLE V
Thermophysical Properties of the Aluminum Alloy at Various Temperatures

Temperature (°C)	0	100	200
Heat conductivity (W/m °C)	160	181	194
Heat capacity (J/kg °C)	828	912	967
Density (kg/m^3)	2700	2700	2700

using a thermocouple. Figure 8 shows the internal temperature profiles of parts molded with various types of extended surfaces. The processing conditions used were: a weight charge of 200 g, an oven temperature of 270°C, a rotational speed of 12 rpm, and with a still air cooling. All measured temperature profiles exhibited a similar heating/cooling temperature profile with four identifiable stages: induction, adherence of powder, melting-sintering of powder, and fusion-densification.[14,15]

The experimental results in Figure 8 suggest that with the addition of fins the heating time of the rotational molding process is reduced by $\sim$ 14% and the cooling time is reduced by 15%. In addition, the measured results in Figure 8 suggest that the pin fins provided the highest heat transfer rate and molded parts with the least amount of time. This is due to the fact that based on the total volume; the pin fin has the largest total surface area (Table I). The heat transfer rate is increased by increasing the surface area across that which the convection occurs. The pin fin thus heats and cools the mold and part faster. Surprisingly, despite the total surface of the triangular fin being smaller than that of the pin fin, the triangular fin exhibited about the same heating/cooling efficiency as that of the pin fin. This may be due to the assumption that the entire potential heat transfer surface has been fully utilized in the fins. For pin fins, part of the surfaces, especially the surfaces that face the opposite direction of the airflow, may not be exposed very well to the air. On the contrary, based on the rotating direction of the mold, the surfaces of the triangular fins were fully utilized (see Fig. 2). Triangular fins thus exhibit similar efficiency as that of pin fins.

During rotational molding, the mold exterior surface is completely exposed to the air. In the oven, the mold and the resin are heated by forced convection of hot air. Therefore, according to the heat transfer theory, the heat transfer rate at the free surface of the metal mold will depend on the temperature gradient of the mold surface temperature and the oven temperature. Furthermore, the selection of a particular fin configuration may depend on space, weight, manufacturing, and cost consideration, as well as on the extent to which the fins reduce the surface convection coefficient and increase the pressure drop associated with flow over the fins.[11] Theoretically, fins are used to increase the heat transfer from a surface by increasing the effective surface area. However, the fin itself represents a conduction resistance to heat transfer from the original surface. In addition, the significant potential improvements in convective heat transfer can be offset by the increased amount of energy that is stored, and subsequently removed from the mold. For these reasons, there is no assurance that the heat transfer rate will be increased through the use of fins. Fin effectiveness can be enhanced by the choice of a material of high thermal conductivity. Aluminum alloys and copper come to mind. However, although copper is superior from the standpoint of thermal conductivity, aluminum alloys are the more common choice because of additional benefits related to lower cost and weight. Fin effectiveness is also enhanced by increasing the ratio of the perimeter to the cross-sectional area. For this reason, the use of thin, but closed spaced fins is preferred, with the provison that the fin gap not be reduced to a value for which flow between the fins is severely impeded, thereby reducing the convection coefficient.[11]

In this study, the pin fin was found to best enhance the heat transfer rate. Nevertheless, its advantage is offset by a high manufacturing cost. Hence, a straight triangular fin is more attractive because for a given equivalent heat transfer, it requires much less volume (fin materials) than that of a rectangular profile.[11] In addition, it should be noted that a still air cooling was used to cool the mold in this study. When water spay cooling was used, the cooling efficiency of the enhanced surfaces was found to be significantly reduced. A detailed comparison of the effects of various processing conditions on the fins performance will be completed and published in future articles.

TABLE VI
Thermophysical Properties of the Air at Different Temperatures

Temperature (°C)	−23	27	77	127	177	227
Heat conductivity (W/m °C)	22.3×10^{-3}	26.3×10^{-3}	30×10^{-3}	33.8×10^{-3}	37.3×10^{-3}	40.7×10^{-3}
Heat capacity (J/kg °C)	1006	1007	1009	1014	1021	1030
Density (kg/m^3)	1.3947	1.1614	0.995	0.8711	0.7740	0.6964

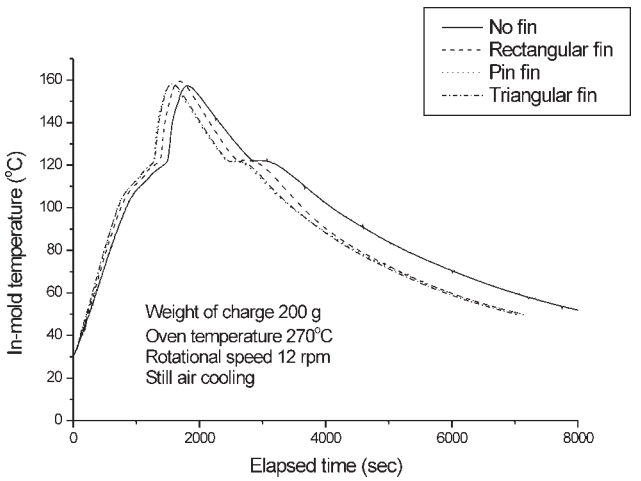

Figure 8 Measured internal air temperature profiles for parts rotationally molded by various fins.

Heating and cooling simulations

To cross reference the validity of the transient heat transfer model proposed in this study, the model was used to calculate the temperature profile of the internal air and compared to the empirical data. Figure 9(a–d) show the results. The match between numerical and experimental results is good in the early stages of the process (powder heating and melting). However, the two deviate from each other in the later stages (heating of polymer melt and melt crystallization). The calculated in-mold air temperatures for all fins are lower than the measured temperatures during the cooling process.

There are at least three factors that might affect the agreement between the numerical and experimental results shown in Figure 9(a–d). The first one is that in the simulation, a simplified model for the polyethylene phase change was used, i.e., a single melting temperature at which all of the latent heat was absorbed. In reality, the powder melts gradually and the powder/melt interface moves and this movement may affect the heat transfer rate at different times. Second, in the simulation it was assumed that all polymer powders remain stagnant during the heating process. However, in reality the powder tumbles inside the mold before it is completely

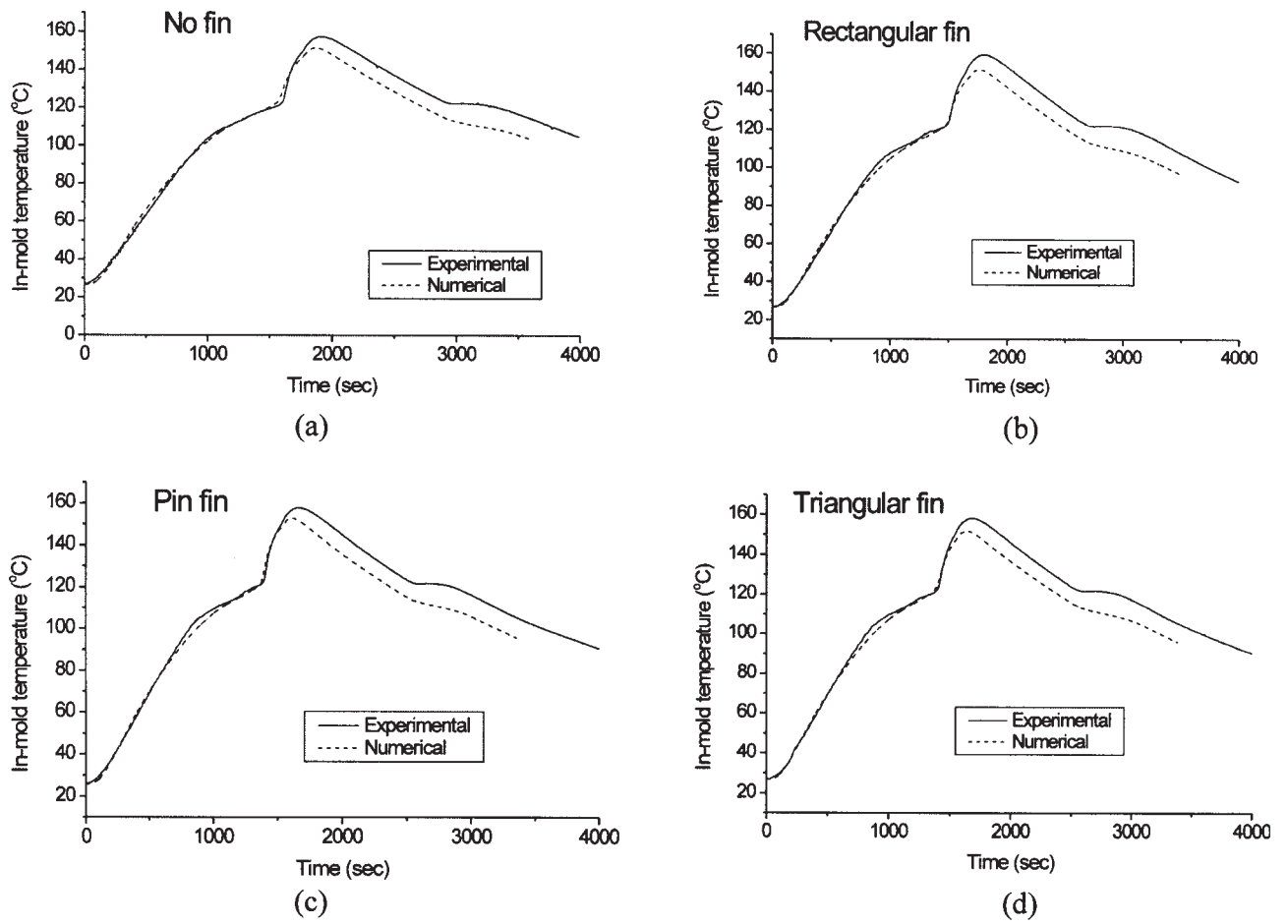

Figure 9 Comparison of the numerical result and experimental data for parts molded by (a) without fin, (b) rectangular fin, (c) pin fin, and (d) triangular fin.

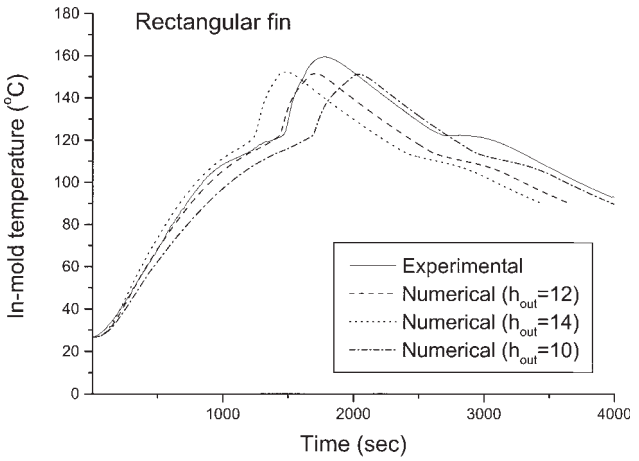

Figure 10 Effects of the values of heat transfer coefficients on the simulated temperature profiles in rotational molding.

melted. A possible third factor affecting the agreement pertains to the significant potential improvements in convective heat transfer that can be offset by the increased amount of energy that is stored, and that can be subsequently removed from the mold during the cooling process. It will provide extra heat sources for the cooling of the mold and lead to a slower cooling of the mold, i.e., a time delay. Nevertheless, in the numerical simulation, the cooling is assumed to start once the heating process ends. This may explain why the numerical results deviate from the experimental results in the later stages (during the cooling process). Overall, when compared to the experimental data, the transient heat transfer model predicted well the temperature profiles of rotationally molded parts. The results testify to the validity of the current transient heat transfer model for the prediction of the heating and cooling process of rotational molding enhanced with fins.

It should be noted that while under the best of circumstances the values of heat transfer coefficients inside and outside are poorly known, they play important roles in affecting the numerical results. The effects of the h values on the simulated temperature profiles were examined by conducting a simple parametric study using different values of $\overline{h}_{ext}$ (10, 12 and 14 W/m^2 °C; the 12 W/m^2 °C one was the value used in this analysis). The simulated results in Figure 10 suggest that the values of heat transfer coefficients indeed have significant influence on the numerical simulation of the heating/cooling cycles of rotationally molded parts. This further testifies that an accurate value of heat transfer coefficient is highly desired for the numerical simulation of rotational molding cycle.

Finally, the surface/volume increase seen with the addition of fins/pins is only one factor in the increase in the rate at which heat is transferred. The air flow patterns around the mold are affected by the position of the fins and their geometry and affect the heat transfer. On the other hand, this study has proposed an unsteady-state, nonlinear heat transfer model to numerically simulate the internal air temperature profiles. The results of this study will enable prediction of the heating and cooling time of rotational molding enhanced with fins, and hence the overall cycle time for the process. On the basis of the experimental results on an empty mold, one can predict the optimal arrangement of fins. In addition, by using the finite element model,[12] one will also be able to predict how the enhancing fins affect when the process is scaled up.

CONCLUSIONS

This report has investigated, both experimentally and numerically, the heating/cooling process of rotational molds enhanced with fins. Rotational molding experiments were carried out in a laboratory scale uniaxial machine, which is capable of measuring internal air temperature in the cycle. Three types of fin-enhanced molds, including pin, rectangular, and triangular fins, were used to mold the parts. It was found that the mold surface enhanced with pins exhibited the highest heating and cooling efficiency. Nevertheless, from a design perspective, ease of manufacturing also needs to be taken into account which could make triangular fin geometry other than pins a better choice to enhanced heat transfer. In addition, an unsteady-state, nonlinear heat transfer model of the rotational molding has been proposed to numerically simulate the internal air temperature profiles. The model parameters are determined from differential scanning calorimetry measurements. It is shown that the numerical predictions are in good agreement with experimental data. This model enables prediction of the heating time and cooling time of rotational molding enhanced with fins, and hence the overall cycle time for the process. This would provide significant advantages in terms of reduced cycle time and improved product quality.

NOMENCLATURE

T	temperature
ρ	material density
C_p	heat capacity
k	heat conductivity
Q	volumetric heat source
T	time
[C]	heat capacitance matrix
[K]	heat conductance matrix
q	surface heat flux

$\{F_v\}$	thermal load from volumetric heat source
$\{F_s\}$	thermal load matrix from surface heat flux
Θ	= 0 fully explicit, = 1 fully implicit scheme
[N]	shape function
[B]	shape function derivative
$\overline{h}_{int}$	heat convection coefficient between the polymer melt and the in-mold air
$\overline{h}_{ext}$	heat convection coefficient between the mold and the outside air
Vp	volumetric percentage
H	enthalpy

References

1. Crawford, R. J. Rotational Molding of Plastics. Wiley: New York, 1992.
2. Xin, W.; Harkin-Jones, E. H.; Crawford, R. J.; Fatnes, A.-M. Plast Rubber Compos 2000, 29, 340.
3. Kontopoulou, M.; Bisaria, M.; Vlachopoulos, J. Int Polym Process 1997, 12, 165.
4. Torres, F. G.; Aragon, C. L. Polym Test 2006, 25, 568.
5. Liu, S. J.; Tsai, C. H. Polym Eng Sci 1999, 39, 1776.
6. Liu, S. J.; Ho, C. Y. Adv Polym Technol 1999, 18, 201.
7. Abdullah, M. Z.; Bickerton, S.; Bhattacharyya, D. Polym Eng Sci 2005, 45, 114.
8. Greco, A.; Maffezzoli, A.; Vlachopoulos, J. Adv Polym Technol 2003, 22, 271.
9. Xu, L.; Crawford, R. J. Plast Rubber Compos 1994, 21, 257.
10. Olson, L. G.; Crawford, R.; Kearns, M.; Geiger, N. Polym Eng Sci 2000, 40, 1758.
11. Incropera, F. P.; Dewitt, D. P. Fundamental of Heat and Mass Transfer, 5th ed.; Wiley: New York, 2001.
12. Cook, R. D.; Malkus, D. S.; Plesha, M. E. Concepts and Applications of Finite Element Analysis, 3rd ed.; Wiley: New York, 1989.
13. Hughes, T. J. R. The Finite Element Method; Prentice-Hall: New Jersey, 1987.
14. Bellehumeur, C. T.; Kontopoulou, M.; Vlachopoulos, J. Rheol Acta 1998, 37, 270.
15. Liu, S. J. Int Polym Process 1998, 13, 88.